GEOPHYSICS, VOL. 76, NO. 4 (JULY-AUGUST 2011); P. L29–L34, 3 FIGS.
10.1190/1.3587221

Potential fields and their partial derivatives produced by a 2D homogeneous polygonal source: A summary with some revisions

Zhen Jia[1] and Shiguo Wu[1]

ABSTRACT

We summarized and revised the present forward modeling methods for calculating the gravity- and magnetic-field components and their partial derivatives of a 2D homogeneous source with a polygonal cross section. The responses of interest include the gravity-field components and their first- and second-order partial derivatives and the magnetic-field components and their first-order partial derivatives. The revised formulas consist of several basic quantities that are common in all the formulations. A singularity appears when the observation point coincides with a polygon vertex. This singularity is removable for the gravity formulas but not for the others. The compact forms of the revised formulas make them easy to implement. We compare the gravity- and magnetic-field components and their partial derivatives produced by a 2D prism whose polygonal cross section approximates a cylinder with the corresponding analytical fields and partial derivatives of the cylinder. The perfect fittings presented by both data sets confirm the reliability of the updated formulas.

INTRODUCTION

A linear geologic structure, when its strike extension is far greater than its cross-section dimension (Grant and West, 1965) and its physical properties (e.g., density, susceptibility, and remanent magnetization) do not vary distinctively, can be approximated by a 2D homogeneous body with infinite length and an invariant cross-section shape. Hubbert (1948) first introduced the line-integral forms of the vertical gravity-field component produced by a 2D source. Talwani et al. (1959) started from the line integrals of the gravity-field components to derive the analytical formulas to calculate the gravity field generated by a 2D homogeneous source with a polygonal cross section. Several years later, Talwani and Heirtzler (1964) proposed the magnetic formulas for a 2D source. The original gravity formulas given by Talwani et al. (1959) have seven special cases, which make them very tedious. The gravity and magnetic formulas given by Talwani and Heirtzler (1964) are not applicable if the polygon border crosses over the discontinuity of the angular quantity as explained later. These limitations make the algorithms inconvenient, especially for programming. Won and Bevis (1987) noticed this problem and updated the gravity formulas; furthermore, they used Poisson's relation to derive the magnetic formulas. However, these gravity and magnetic formulas can be further revised to make them simpler and more compact because they contain some redundant terms that can be eliminated; these terms sum up to zero over a closed polygon. Because of its simplicity and versatility, the polygonal prism became a standard of 2D forward modeling. In recent years, the magnetic gradiometry has been an area of growing interest. Jia and Meng (2009) proposed a set of formulas to compute the partial derivatives of the magnetic-field components generated by a 2D homogeneous source. For a comprehensive review of forward modeling methods, one could refer to the introductory part of the papers by Nabighian et al. (2005a, 2005b). Our goal is to supply a "quick reference" to interpreters or software developers to build interactive computer programs by themselves. The idea to express gravity and magnetic fields with common basic quantities is not new. Holstein (2002a, 2002b) used the term "gravimagnetic similarity" to describe the reappearance of a vector function associated with the facet edges of uniform polyhedra in the Newtonian potential, gravity-field components (or magnetic potential), and gravity-gradient components (or magnetic-field components) produced by such a source. This is an effort in a 3D context to obtain forward formulas with unified style and compact formulation, whereas our paper focuses on 2D methods. To avoid confusion, we use the term "magnetic field" to denote the magnetic flux density, namely, the "B field," and we follow a traditional

Manuscript received by the Editor 19 July 2010; revised manuscript received 23 January 2011; published online 7 June 2011.
[1]Chinese Academy of Sciences, Institute of Oceanology, Key Laboratory of Marine Geology and Environment, Qingdao, China. E-mail: chiachen@qdio.ac.cn; swu@qdio.ac.cn.

treatment to assume that the magnetic source is uniformly magnetized and the anomalous field is much smaller than the ambient field.

PARTIAL DERIVATIVES OF THE NEWTONIAN POTENTIAL

The Newtonian potential of a 2D homogeneous source, namely, the logarithmic potential, is defined as (see Blakely, 1995, p. 58)

$$U(x,z) = 2G\rho \iint\limits_S \log\frac{1}{r}\, dx_s dz_s, \tag{1a}$$

where

$$r = \sqrt{(x_s - x)^2 + (z_s - z)^2} \tag{1b}$$

is the distance between the observation point (x, z) and the source point (x_s, z_s), G is gravitational constant, ρ is the source density, and S is the cross section of the source. Here we assume that the strike of the 2D source is parallel to the y-axis; hence, the integral of the right-hand side of equation 1a is independent of y, namely,

$$\frac{\partial U}{\partial y} = 0. \tag{2}$$

Therefore, Laplace's equation reduces to

$$\nabla^2 U = \frac{\partial^2 U}{\partial x^2} + \frac{\partial^2 U}{\partial z^2} = 0, \tag{3}$$

and Poisson's relation (see Blakely, 1995, p. 92) between the scalar magnetic potential V and the Newtonian potential U of a 2D homogeneous source,

$$V = -\frac{\mu_0}{4\pi G\rho}\mathbf{M}\cdot\nabla U, \tag{4}$$

reduces to

$$V = -\frac{\mu_0}{4\pi G\rho}\left(M_x\frac{\partial U}{\partial x} + M_z\frac{\partial U}{\partial z}\right), \tag{5}$$

where μ_0 in equations 4 and 5 represents vacuum permeability and the vector $\mathbf{M}$ in equation 4 and the scalars M_x and M_z in equation 5 represent the magnetization vector and its x- and z-components, respectively. Beginning with equations 1a, 2, 3, and 5, we can express the quantities of interest in this paper by the first- to third-order partial derivatives of the logarithmic potential as follows.

The gravity-field components are

$$g_x = \frac{\partial U}{\partial x} \tag{6a}$$

$$g_z = \frac{\partial U}{\partial z}. \tag{6b}$$

The gravity-gradient components are

$$\frac{\partial g_x}{\partial x} = -\frac{\partial g_z}{\partial z} = \frac{\partial^2 U}{\partial x^2} \tag{7a}$$

$$\frac{\partial g_x}{\partial z} = \frac{\partial g_z}{\partial x} = \frac{\partial^2 U}{\partial x\partial z}. \tag{7b}$$

The second-order partial derivatives of the gravity-field components are

$$\frac{\partial^2 g_x}{\partial x^2} = -\frac{\partial^2 g_x}{\partial z^2} = -\frac{\partial^2 g_z}{\partial x\partial z} = \frac{\partial^3 U}{\partial x^3} \tag{8a}$$

$$\frac{\partial^2 g_x}{\partial x\partial z} = \frac{\partial^2 g_z}{\partial x^2} = -\frac{\partial^2 g_z}{\partial z^2} = \frac{\partial^3 U}{\partial x^2\partial z}. \tag{8b}$$

The magnetic-field components are

$$B_x = \frac{\mu_0}{4\pi G\rho}\left(M_x\frac{\partial^2 U}{\partial x^2} + M_z\frac{\partial^2 U}{\partial x\partial z}\right) \tag{9a}$$

$$B_z = \frac{\mu_0}{4\pi G\rho}\left(M_x\frac{\partial^2 U}{\partial x\partial z} - M_z\frac{\partial^2 U}{\partial x^2}\right). \tag{9b}$$

The magnetic-gradient components are

$$\frac{\partial B_x}{\partial x} = -\frac{\partial B_z}{\partial z} = \frac{\mu_0}{4\pi G\rho}\left(M_x\frac{\partial^3 U}{\partial x^3} + M_z\frac{\partial^3 U}{\partial x^2\partial z}\right) \tag{10a}$$

$$\frac{\partial B_x}{\partial z} = \frac{\partial B_z}{\partial x} = \frac{\mu_0}{4\pi G\rho}\left(M_x\frac{\partial^3 U}{\partial x^2\partial z} - M_z\frac{\partial^3 U}{\partial x^3}\right). \tag{10b}$$

When the magnitude of the anomalous field is small enough compared to the magnitude of the ambient geomagnetic field, the scalar total field magnetic anomaly could be expressed as

$$\Delta T = B_x\cos I\sin(A-D) + B_z\sin I,\ A\in[0,2\pi). \tag{11}$$

Here D and I are the declination and inclination of the geomagnetic field, respectively, and A is the azimuth of the positive y, which is parallel to the strike of the source (Figure 1). As a correction to equation 20 in the paper by Jia and Meng (2009), Equation 11 is applicable for the whole x-y-plane, with a redefinition of the angle A, whereas Jia and Meng's equation 20 fails when the positive y-axis lies on the east half plane. Substituting the x- and z-components of the magnetic field, equations 9a and 9b, into equation 11, the expression of the scalar total field magnetic anomaly becomes

$$\Delta T = C_1\frac{\partial^2 U}{\partial x^2} + C_2\frac{\partial^2 U}{\partial x\partial z}, \tag{12a}$$

where

$$C_1 = \frac{\mu_0}{4\pi G\rho}[M_x\cos I\sin(A-D) - M_z\sin I] \tag{12b}$$

$$C_2 = \frac{\mu_0}{4\pi G\rho}[M_x\sin I + M_z\cos I\sin(A-D)]. \tag{12c}$$

Differentiating equation 12a with respect to x and z and applying Laplace's equation (equation 3), we obtain the partial derivatives

$$\frac{\partial \Delta T}{\partial x} = C_1\frac{\partial^3 U}{\partial x^3} + C_2\frac{\partial^3 U}{\partial x^2\partial z} \tag{13a}$$

$$\frac{\partial \Delta T}{\partial z} = C_1\frac{\partial^3 U}{\partial x^2\partial z} - C_2\frac{\partial^3 U}{\partial x^3}. \tag{13b}$$

It is quite clear by examining equations 6a–10b, 12a, 13a, and 13b that the gravity- and magnetic-field components and their partial derivatives are expressed in terms of the first- to third-order partial derivatives of the logarithmic potential, which make up the set

$$\left\{\frac{\partial U}{\partial x},\frac{\partial U}{\partial z},\frac{\partial^2 U}{\partial x^2},\frac{\partial^2 U}{\partial x\partial z},\frac{\partial^3 U}{\partial x^3},\frac{\partial^3 U}{\partial x^2\partial z}\right\}. \quad (14)$$

FORMULAS FOR CALCULATING THE FIELDS AND THEIR PARTIAL DERIVATIVES

For a cross section of arbitrary shape, the partial derivatives in set 14 are very hard to evaluate. The traditional treatment approximates the arbitrary shape with a polygon because the integrations with respect to such a shape are very easy to evaluate. We give an outline of this process below.

First-order partial derivatives

The first-order partial derivatives of the logarithmic potential are exactly the gravity-field components, and following Hubbert (1948) and Talwani et al. (1959), they can be expressed as line integrals,

$$\frac{\partial U}{\partial x}=2G\rho\oint_L r\cos\theta d\theta \quad (15a)$$

$$\frac{\partial U}{\partial z}=2G\rho\oint_L r\sin\theta d\theta, \quad (15b)$$

where θ is the clockwise angle from positive x-axis direction to the source point (x_s, z_s) and the clockwise integration path L is the boundary of the integration area S (Figure 2). For a 2D source with a polygonal cross section, we can express the line integrals in equations 15a and 15b as

$$\oint_L r\cos\theta d\theta=\sum_i\int_{L_i} r\cos\theta d\theta \quad (16a)$$

$$\oint_L r\sin\theta d\theta=\sum_i\int_{L_i} r\sin\theta d\theta. \quad (16b)$$

Here L_i denotes the ith segment of the polygon boundary L (Figure 2). The results of the integrations are

$$\int_{L_i} r\cos\theta d\theta=r_i\sin(\theta_i-\varphi_i)\left(-\cos\varphi_i\log\frac{r_{i+1}}{r_i}-\sin\varphi_i\Delta\theta_i\right) \quad (17a)$$

$$\int_{L_i} r\sin\theta d\theta=r_i\sin(\theta_i-\varphi_i)\left(-\sin\varphi_i\log\frac{r_{i+1}}{r_i}+\cos\varphi_i\Delta\theta_i\right), \quad (17b)$$

where

$$\Delta\theta_i=\begin{cases}\theta_{i+1}-\theta_i+2\pi & (\theta_{i+1}-\theta_i<-\pi),\\ \theta_{i+1}-\theta_i & (-\pi\le\theta_{i+1}-\theta_i\le\pi),\\ \theta_{i+1}-\theta_i-2\pi & (\theta_{i+1}-\theta_i>\pi).\end{cases} \quad (17c)$$

Here (r_i, θ_i) and (r_{i+1}, θ_{i+1}) are polar coordinates corresponding to the ith and (i+1)th vertices of the polygonal cross section S, respectively, and φ_i is the slope angle of the segment L_i (Figure 2). Equation 17c is equivalent to, but much simpler than, case 1 of Won and Bevis (1987). The jumps of $\Delta\theta_i$ are attributed to integration over the 0/2π discontinuity of angle θ (see appendix for detailed comments). A singularity occurs when $r_i=0$ or $r_{i+1}=0$, which represents a juxtaposition of the observation point with the polygon vertices. However, it is very easy to prove by applying

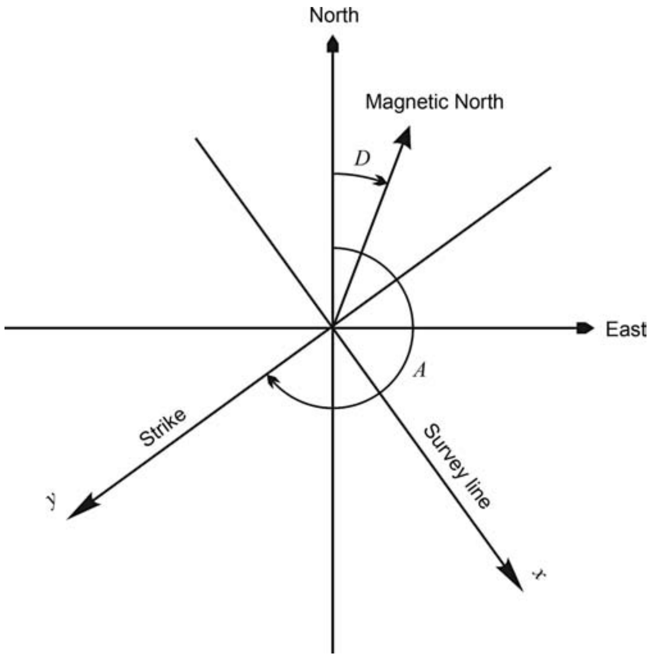

Figure 1. Schematic plan view of a 2D structure with its strike parallel to the y-axis. The measurement profile is along the x-axis. A is the azimuth of the positive y-axis, and D is the geomagnetic declination.

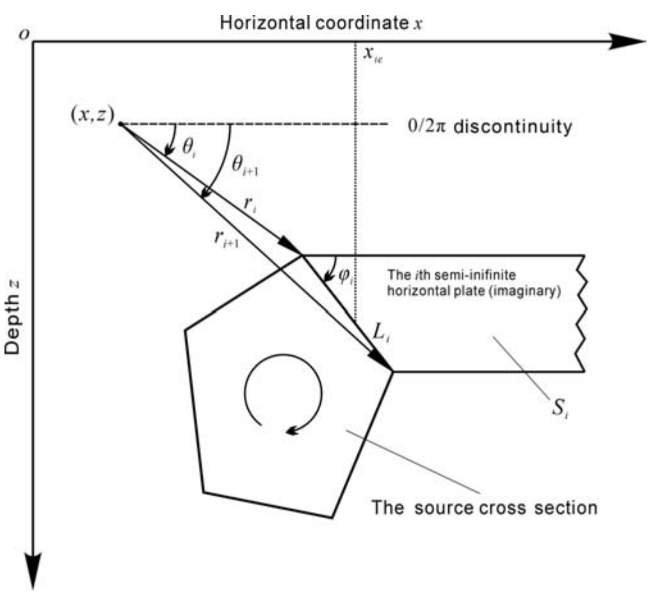

Figure 2. Cross section of a 2D horizontal polygonal source on the x-z-plane. Each edge of the polygon corresponds to an imaginary horizontal semi-infinite plate. The rotation arrow inside the polygon indicates a clockwise integration path.

L'Hôpital's rule that the integrals on the left-hand side of equations 17a and 17b become zero when this happens.

Second- and third-order partial derivatives

The derivation process of the second- and third-order partial derivatives of the logarithmic potential follows the same strategy that Talwani and Heirtzler (1964) used to derive the magnetic formulas. The integrations over the cross-section area S can be evaluated indirectly as summations:

$$\frac{\partial^2 U}{\partial x^2} = -2G\rho \sum_i \int_{z_i}^{z_{i+1}} dz_s \int_{x_{ie}}^{\infty} \frac{\partial^2}{\partial x^2}\left(\log\frac{1}{r}\right) dx_s, \quad (18a)$$

$$\frac{\partial^2 U}{\partial xz} = -2G\rho \sum_i \int_{z_i}^{z_{i+1}} dz_s \int_{x_{ie}}^{\infty} \frac{\partial^2}{\partial x \partial z}\left(\log\frac{1}{r}\right) dx_s, \quad (18b)$$

$$\frac{\partial^3 U}{\partial x^3} = -2G\rho \sum_i \int_{z_i}^{z_{i+1}} dz_s \int_{x_{ie}}^{\infty} \frac{\partial^3}{\partial x^3}\left(\log\frac{1}{r}\right) dx_s, \quad (18c)$$

$$\frac{\partial^3 U}{\partial x^2 \partial z} = -2G\rho \sum_i \int_{z_i}^{z_{i+1}} dz_s \int_{x_{ie}}^{\infty} \frac{\partial^3}{\partial x^2 \partial z}\left(\log\frac{1}{r}\right) dx_s. \quad (18d)$$

Here x_{ie} (the subscript e indicates edge) is the abscissa of an arbitrary point on the polygon border L_i. Every integral on the right-hand sides of equations 18a–18d corresponds to a semi-infinite horizontal plate denoted by the symbol S_i (Figure 2). The effect of the imaginary source outside the real source will cancel out in a clockwise summation process. The minus sign is necessary to get correct results. The results of the integrations are

$$\int_{z_i}^{z_{i+1}} dz_s \int_{x_{ie}}^{\infty} \frac{\partial^2}{\partial x^2}\left(\log\frac{1}{r}\right) dx_s = \sin\varphi_i \left(\cos\varphi_i \log\frac{r_{i+1}}{r_i} + \sin\varphi_i \Delta\theta_i\right), \quad (19a)$$

$$\int_{z_i}^{z_{i+1}} dz_s \int_{x_{ie}}^{\infty} \frac{\partial^2}{\partial x \partial z}\left(\log\frac{1}{r}\right) dx_s = \sin\varphi_i \left(\sin\varphi_i \log\frac{r_{i+1}}{r_i} - \cos\varphi_i \Delta\theta_i\right), \quad (19b)$$

$$\int_{z_i}^{z_{i+1}} dz_s \int_{x_{ie}}^{\infty} \frac{\partial^3}{\partial x^3}\left(\log\frac{1}{r}\right) dx_s = \left(\frac{\sin\theta_{i+1}}{r_i} - \frac{\sin\theta_i}{r_{i+1}}\right)\cos(\theta_i + \theta_{i+1}), \quad (19c)$$

$$\int_{z_i}^{z_{i+1}} dz_s \int_{x_{ie}}^{\infty} \frac{\partial^3}{\partial x^2 \partial z}\left(\log\frac{1}{r}\right) dx_s = \left(\frac{\sin\theta_{i+1}}{r_i} - \frac{\sin\theta_i}{r_{i+1}}\right)\sin(\theta_i + \theta_{i+1}). \quad (19d)$$

Here the quantity $\Delta\theta_i$ (equations 19a and 19b) is the same one defined in Equation 17c. A singularity occurs when $r_i = 0$ or $r_{i+1} = 0$, but this time it is an infinite singularity. Equations 19a and 19b are much simpler compared with the results given by Won and Bevis (1987), and equations 19c and 19d have the same singularity as the formulas shown by Jia and Meng (2009).

Finally, according to equations 16a–19d, we get the equations of the first- to third-order partial derivatives of the logarithmic potential as

$$\frac{\partial U}{\partial x} = 2G\rho \sum_i r_i \sin(\theta_i - \varphi_i)\left(-\cos\varphi_i \log\frac{r_{i+1}}{r_i} - \sin\varphi_i \Delta\theta_i\right), \quad (20a)$$

$$\frac{\partial U}{\partial z} = 2G\rho \sum_i r_i \sin(\theta_i - \varphi_i)\left(-\sin\varphi_i \log\frac{r_{i+1}}{r_i} + \cos\varphi_i \Delta\theta_i\right), \quad (20b)$$

$$\frac{\partial^2 U}{\partial x^2} = 2G\rho \sum_i \sin\varphi_i \left(-\cos\varphi_i \log\frac{r_{i+1}}{r_i} - \sin\varphi_i \Delta\theta_i\right), \quad (20c)$$

$$\frac{\partial^2 U}{\partial xz} = 2G\rho \sum_i \sin\varphi_i \left(-\sin\varphi_i \log\frac{r_{i+1}}{r_i} + \cos\varphi_i \Delta\theta_i\right), \quad (20d)$$

$$\frac{\partial^3 U}{\partial x^3} = 2G\rho \sum_i \left(\frac{\sin\theta_i}{r_{i+1}} - \frac{\sin\theta_{i+1}}{r_i}\right)\cos(\theta_i + \theta_{i+1}), \quad (20e)$$

$$\frac{\partial^3 U}{\partial x^2 \partial z} = 2G\rho \sum_i \left(\frac{\sin\theta_i}{r_{i+1}} - \frac{\sin\theta_{i+1}}{r_i}\right)\sin(\theta_i + \theta_{i+1}). \quad (20f)$$

We can find by comparing equation 20a with 20c and 20b with 20d that common parts (the terms inside the last parentheses of each equation) recover after a differentiation operation. This phenomenon is consistent with the gravimagnetic similarity described by Holstein (2002a, 2002b). Substituting the first- to third-order partial derivatives of the logarithmic potential, equations 20a–20f, into equations 6a–10b, 12a, 13a and 13b, respectively, we can get the analytic formulas to calculate the potential fields and their partial derivatives generated by a 2D homogenous polygonal source. The algorithms for calculating the first-order partial derivatives of the magnetic-field components are virtually the same as those given by Jia and Meng (2009), except that we made a modification to the suffixes and use polar instead of the Cartesian coordinates.

SYNTHETIC EXAMPLE

To test the reliability of the revised formulas, we compared the gravity- and magnetic-field components and their partial derivatives generated analytically by a 2D horizontal cylinder with the corresponding responses computed using the formulas presented in this paper and produced by a regular polygonal prism inscribing the cylinder. The Newtonian potential of a uniform horizontal cylinder with a radius a of its cross section is given by (Blakely, 1995, p. 57)

$$U = 2\pi a^2 G\rho \log\frac{1}{r}. \quad (21)$$

Substituting the form Equation 21 of the Newtonian potential into equations 6a–10b, 12a, 13a and 13b, we can deduce the

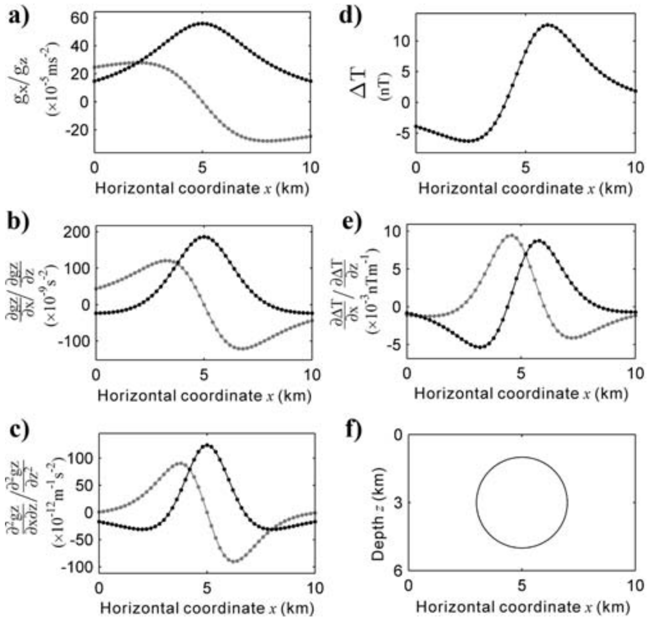

Figure 3. Comparison of two data sets. One of the data sets (solid lines) is generated analytically by a 2D horizontal cylinder, and the other one (dots), computed by our formulas, is generated by a 2D prism with a polygonal cross section that approximately describe the cylindrical cross section. Gray and black represent components or partial differentiation along x- and z-axes, respectively. (a) The gravity-field components and the (b) first-order and (c) second-order partial derivatives of its vertical component g_z and (d) the magnetic scalar total field anomaly ΔT and (e) its first-order partial derivatives and (f) the cross section of the cylindrical source on the x-z-plane.

formulas for the gravity- and magnetic-field components and their partial derivatives. In this way, we approximate the cylindrical cross section, whose radius is 2 km and whose center is at $x = 5$ km and $z = 3$ km, by a polygonal cross section with 500 vertices. The density and susceptibility of the source are 1000 kg/m^3(1 g/cm^3) and 0.001, respectively. The azimuth of the positive y-axis (parallel to the source strike) $A = 220°$. The ambient magnetic intensity is 50,000 nT, and the declination D and the inclination I of the geomagnetic field are $-6°$ and $53°$, respectively. We set the horizontal and vertical components of the remanent magnetization to be -0.01 and 0.02 A/m, respectively. The gravity and magnetic data are computed on the plane $z = 0$ km along a profile length of 10 km where the data points are sampled in a regular interval of 0.2 km. Figure 3 shows the gravity- and magnetic-field components and their partial derivatives generated by the prism (dots) and the cylinder (solid lines). The good agreement between the two sets of data is obvious.

CONCLUSIONS AND SUGGESTIONS

We have summarized and revised the current 2D forward methods of potential fields and their partial derivatives in this paper. To achieve this aim, we reduced the derivation process to the formulations of the first- to third-order partial derivatives of the logarithmic potential. The updated formulas consist of several common basic quantities, which make them compact and easy to implement by a computer programmer. A singularity, which is removable for the gravity field formulas but not for the others, occurs when the observation point coincides with the polygon vertices. A 2D model cannot approximate a linear geologic body very well when the strike extension of the geologic body is not far greater than its cross-section dimension. Under such circumstances, the end effects of the body cannot be ignored; therefore, a 2.5D model is a better alternative. Historically, several algorithms have been proposed for this kind of model. A review and even new developments, such as magnetic-gradient formulas, for which we have not found detailed and specialized descriptions in the literature, of these algorithms will supply further convenience for building profile-based forward modeling software.

ACKNOWLEDGMENTS

Thanks are owed to Edson Sampaio, Afif Saad, Horst Holstein, and an anonymous reviewer and the Associate Editor, Valéria C. F. Barbosa, for their help in improving the quality of our manuscript. Our work is supported by China Postdoctoral Science Foundation (No. 20090461268), Map Series of Geology and Geophysics of China Seas and Lands (GZH200900504), and Open Research Fund (MGE2009KG01) of Key Laboratory of Marine Geology and Environment of Chinese Academy of Sciences.

APPENDIX A

DETAILED EXPLANATION OF EQUATION 17C

We take as an example the integrals on the right-hand side of equation 16a. For the convenience of the following discussion, we define

$$I_i = \int_{L_i} r \cos\theta d\theta. \tag{A-1}$$

When segment L_i with polygon vertices P_i and P_{i+1} as endpoints (Figure A-1) does not cross over the $0/2\pi$ discontinuity of angle θ (Figure 2), the integration in equation A-1 becomes

$$I_i = \int_{\theta_i}^{\theta_{i+1}} r(\theta) \cos\theta d\theta, \tag{A-2}$$

and such a circumstance corresponds to the inequality

$$-\pi \le \theta_{i+1} - \theta_i \le \pi. \tag{A-3}$$

The integration result is

$$I_i = r_i \sin(\theta_i - \varphi_i) \times \left[\cos\varphi_i \log\left|\frac{\sin(\theta_{i+1} - \varphi_i)}{\sin(\theta_i - \varphi_i)}\right| - \sin\varphi_i(\theta_{i+1} - \theta_i)\right], \tag{A-4}$$

which, by applying sine theorem, reduces to

$$I_i = r_i \sin(\theta_i - \varphi_i)\left[-\cos\varphi_i \log\frac{r_{i+1}}{r_i} - \sin\varphi_i(\theta_{i+1} - \theta_i)\right]. \tag{A-5}$$

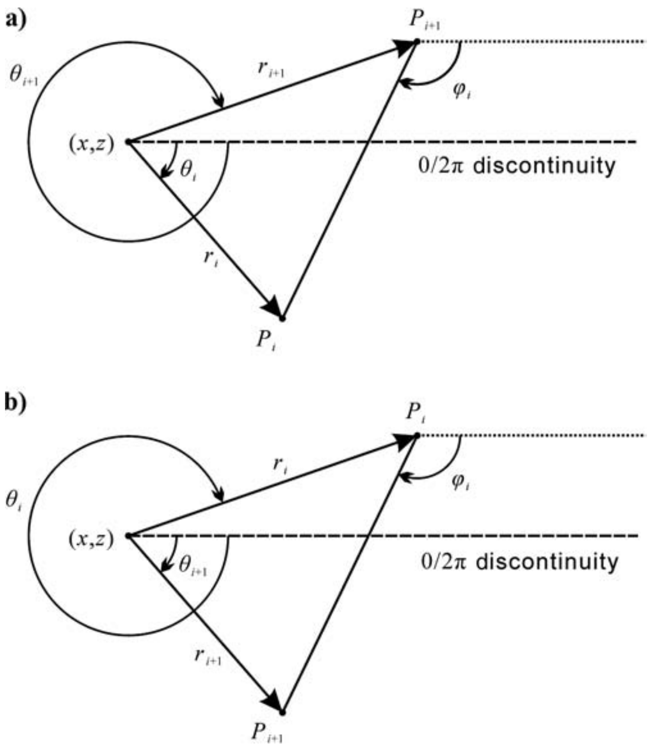

Figure A-1 The case where integration path L_i crosses over the $0/2\pi$ discontinuity with the angle θ jumping (a) from 0 to 2π and (b) from 2π to 0.

When segment L_i crosses over the $0/2\pi$ discontinuity with the integration variable θ jumping from 0 to 2π (Figure A-1a), the integration in equation A-1 becomes

$$I_i = \int_{\theta_i}^{0} r(\theta)\cos\theta d\theta + \int_{2\pi}^{\theta_{i+1}} r(\theta)\cos\theta d\theta, \tag{A-6}$$

and such a circumstance corresponds to the inequality

$$\theta_{i+1} - \theta_i > \pi. \tag{A-7}$$

The integration result is

$$I_i = r_i \sin(\theta_i - \varphi_i) \times \left[-\cos\varphi_i \log\frac{r_{i+1}}{r_i} - \sin\varphi_i(\theta_{i+1} - \theta_i - 2\pi) \right]. \tag{A-8}$$

If we interchange the position of P_i and P_{i+1} (Figure A-1b) with the angle θ jumping from 2π to 0 at the discontinuity, the integration in equation A-1 becomes

$$I_i = \int_{\theta_i}^{2\pi} r(\theta)\cos\theta d\theta + \int_{0}^{\theta_{i+1}} r(\theta)\cos\theta d\theta, \tag{A-9}$$

and such a circumstance corresponds to the inequality

$$\theta_{i+1} - \theta_i < -\pi. \tag{A-10}$$

The integration result is

$$I_i = r_i \sin(\theta_i - \varphi_i) \times \left[-\cos\varphi_i \log\frac{r_{i+1}}{r_i} - \sin\varphi_i(\theta_{i+1} - \theta_i + 2\pi) \right]. \tag{A-11}$$

Finally, equations A-1 A-3 A-5 A-7 A-8 A-9 and A-10 together validate the correctness of Equation 17c. During the discussion above we assume that $0 \leq \theta < 2\pi$, but we must point out that Equation 17c is valid regardless of where the cut in the angle domain is made. It is very easy to prove, following similar derivation processes, that equation 17c holds for the integrals in equations 16b, 18a, and 18b.

REFERENCES

Blakely, R. J., 1995, Potential theory in gravity and magnetic applications: Cambridge University Press.

Grant, F. S., and G. F. West, 1965, Interpretation theory in applied geophysics: McGraw-Hill Book Co., Inc.

Holstein, H., 2002a, Gravimagnetic similarity in anomaly formulas for uniform polyhedra: Geophysics, **67**, 1126–1133., doi:10.1190/1.1500373

Holstein, H., 2002b, Invariance in gravimagnetic anomaly formulas for uniform polyhedra: Geophysics, **67**, 1134–1137., doi:10.1190/1.1500374

Hubbert, M. K., 1948, A line-integral method of computing the gravimetric effects of two-dimensional masses: Geophysics, **13**, 215–225., doi:10.1190/1.1437395

Jia, Z., and L. Meng, 2009, Magnetic gradients produced by a 2D homogeneous polygonal source: Geophysics, **74**, no. 1, L1–L6., doi:10.1190/1.3008054

Nabighian, M. N., M. E. Ander, V. J. S. Grauch, R. O. Hansen, T. R. LaFehr, Y. Li, W. C. Pearson, J.W. Peirce, J. D. Phillips, and M. E. Ruder, 2005a, Historical development of the gravity method in exploration: Geophysics, **70**, no. 6, 63ND–89ND., doi:10.1190/1.2133785

Nabighian, M. N., V. J. S. Grauch, R. O. Hansen, T. R. LaFehr, Y. Li, J. W. Peirce, J. D. Phillips, and M. E. Ruder, 2005b, The historical development of the magnetic method in exploration: Geophysics, **70**, no. 6, 33ND–61ND., doi:10.1190/1.2133784

Talwani, M., and J. R. Heirtzler, 1964, Computation of magnetic anomalies caused by two dimensional structures of arbitrary shape, *in* G. A. Parks, ed., Computers in the mineral industries: Part 1: Stanford University Publication in Geological Sciences 9, 464–480.

Talwani, M., J. L. Worzel, and M. Landisman, 1959, Rapid gravity computations for two-dimensional bodies with application to the Mendocino submarine fracture zone: Journal of Geophysical Research, **64**, 49–59., doi:10.1029/JZ064i001p00049

Won, I. J., and M. Bevis, 1987, Computing the gravitational and magnetic anomalies due to a polygon: Algorithms and Fortran subroutines: Geophysics, **52**, 232–238., doi:10.1190/1.1442298